Regularities of structure and texture development in austenitic steel during cold rolling and heat treatment

***O. A. Krymskaya**, Cand. Phys.-Math., Associate Professor [1], e-mail: XrayTextureLab@gmail.com;*
***M. G. Isaenkova**, Dr. Phys.-Math., Prof.[1], e-mail: isamarg@mail.ru;*
***V. A. Fesenko**, Lead Engineer [1];*
***R. A. Minushkin**, Engineer, Postgraduate Student [1]*

[1] National Research Nuclear University MEPhI (Moscow, Russia):

The paper studies the regularities of the structure and texture formation in austenitic steel AISI 304 under cold rolling and subsequent heat treatment. Regularities of structure and texture formation depending on the rolling type and deformation degree were established. The ratios of main texture components, the volume fractions and the distortion of the martensite's crystalline lattice were analyzed. It is shown that mechanisms of the austenite → martensite phase transformation in the course of cold rolling may change depending on various deformation schemes, as well as mechanisms of the reverse phase transformation variate under subsequent annealing. Herewith depending on the rolling type and deformation degree, the crystallographic texture formation of the nucleating austenite under the heat treatment can have single component or multi-component character and follows different orientation relations. The more scattered martensite texture after deformation results in the formation of fine-dispersed austenite, which hardens the material keeping a sufficient level of plasticity.

Keywords: austenitic steel, cold rolling, martensite, structure, texture, phase transformations.
DOI: 10.17580/cisisr.2022.02.05

Introduction

Austenitic steels with a high chromium and nickel content belong to the corrosion-resistant materials, and in this connection, they have found wide application in various industries: the pipes manufacturing for various purposes, heat exchangers, muffles, exhaust manifolds, spark plug electrodes, welded vessels etc. Moreover, these steels are also used as cladding for fuel elements in fast neutrons reactors. Therefore, comprehensive information about possible structural, textural and mechanical changes during deformation and heating is quite necessary to prevent emergency conditions of these units. To date it is known that widely used stainless steel AISI 304 is susceptible to austenite ↔ martensite ($\alpha \leftrightarrow \gamma'$) phase transformations (PT) under cold deformation and annealing [1-6]. Moreover, in [7] the $\alpha \leftrightarrow \gamma'$ phase transformations were detected under thermal creep of austenitic steel. Authors revealed following processes during cold rolling, which affect the final structure, texture and properties of this steel: deformation of austenite, strain-induced martensitic transformation, further deformation of martensite and retained austenite.

The mechanisms and orientation relations of $\alpha \leftrightarrow \gamma'$ PT during cold or hot rolling and subsequent annealing had been described in [2–4], where authors pay attention to the stacking faults energy. In [4] it was also found that the austenitic phase under deformation below some critical temperature could undergo various transformations into martensite including intermediate ε-phase.

One problem of this steels class is quite low yield strength of approximately 100-400 MPa resulted from coarse-grained γ-austenite [8, 9]. The rising of strength at the expense of work hardening results in the corrosion resistance reduction due to arising of strain-induced martensite. So, fine-grained strengthening is more acceptable way to improve properties of austenitic steels. Recently, such type of strengthening is implemented via severe plastic deformation and subsequently reversion annealing, which main purpose is to realize the reverse PT a martensite → ultra-fine-grained austenite. Such methods like equal-channel angular pressing or high-pressure torsion or cyclic channel die pressing are quite difficult to use for obtain homogeneous specimen of large sizes, so many authors tried to use more simple modifications of ordinary rolling like asymmetric [8, 10], cryogenic-rolling [9] or combined mechanical processing of the surface [11] to obtain high strength. We further develop such an approach in this work using the longitudinal and cross rolling to rise the strength of austenitic steel.

Despite the available data on the structure, mechanical properties and phase transformations features in austenitic steels under deformation and heat treatment the regularities of reverse martensite → austenite transformation, features of different deformation schemes as well as influence of substructure inhomogeneity are still insufficiently studied. Therefore, the aim of this work is to analyse the texture and structure changes of austenitic steel during cold deformation by the longitudinal and cross rolling following with subsequent heat treatment as well as influence of inhomogeneity of deformed state on PT.

Samples and research methods

We studied samples of austenitic steel subjected to deformation by longitudinal and cross rolling (LR and CR, respectively) and subsequent heat treatment (HT) by the water quenching from 700 °C with different holding times — 1, 5 and 20 minutes before cooling. The starting samples were a commercial stainless steel AISI 304 of 20×20×5 mm in dimensions cut out from a forged rod. The total reduction was ~ 90 % and the final thickness was ~ 0.7 mm. The specified chemical composition of AISI 304 is 0.8 C–18 Cr–10 Ni (wt.%). The diffraction patterns were registered for different deformation degrees and after HT by using X-ray diffractometer DRON-3M with CuK_α radiation and graphite monochromator. It is known that AISI 304 steel may consist of two phases: α'-martensite – interstitial solid solution of α-Fe having body-centered tetragonal (BCT) crystalline lattice and γ-austenite with face-centered cubic (FCC) lattice. We determined with DIFFRAC.TOPAS v.5.0 software the full width at half maximum (FWHM) of the (211) martensite and the (220) austenite reflections for the structure parameters characterization, because the FWHM correlates with the structure fragmentation and microstrains.

As the material has strong texture, the Rietveld refinement for quantitative phase analysis is not applicable. Therefore, we use the following semi-empirical equation from [6] for the α'-martensite volume fraction ($VF_{\alpha'}$) determination (Equation (1)):

$$VF_{\alpha'} = \frac{I_{(211)\alpha'}}{I_{(211)\alpha'} + 0{,}65 \cdot (I_{(311)\gamma} + I_{(220)\gamma})}\,. \qquad (1)$$

The texture pole figures (PFs) were registered on samples' surfaces parallel to the rolling plane (RP) with CrK_α radiation by means of standard procedure [12]. In the case of the dual-phase state of the material, by two experimental PFs were used: {100} and {112} for the α'-phase; {100} and {110} for the γ-phase. In the absence of austenite the additional {110} PF for α'-phase were registered. Then the orientation distribution functions (ODF) $f(g)$ were restored using LaboTexa3.0 software [13]. Texture analysis was implemented by typical for cubic materials three-dimensional ODF cross-sections at constant Euler angle $\varphi_2 = 45°$ in the Bunge notation [14]. As a quantitative texture characteristic we used the volume fractions of different texture components (TVFs), calculated via LaboTex within 10–15 degrees around the appropriate orientation using simple integration method with dividing among overlapping orientations, and so-called texture index T_f, which determined by integrating the ODF squares over the orientation space (g) (Equation (2)):

$$T_f = \oint f(g)^2\, dg \qquad (2)$$

T_f shows the predominance degree of grains of certain orientations in comparison with a material of random texture, for which the detection probability of any grains orientation is uniform and equal to the unity, according to the normalization conditions, while for an ideal single crystal $T_f \to \infty$.

Additionally we measured the microhardness by means of instrumented indentation with DNT 1/5 under load of 1000 mN using Berkovich pyramid. The analyzed parameters were the Meyer hardness (HM) [15] and the plasticity (δ_H) evaluated by the relation of the plastic area under loading diagram to the maximum area [16, 17].

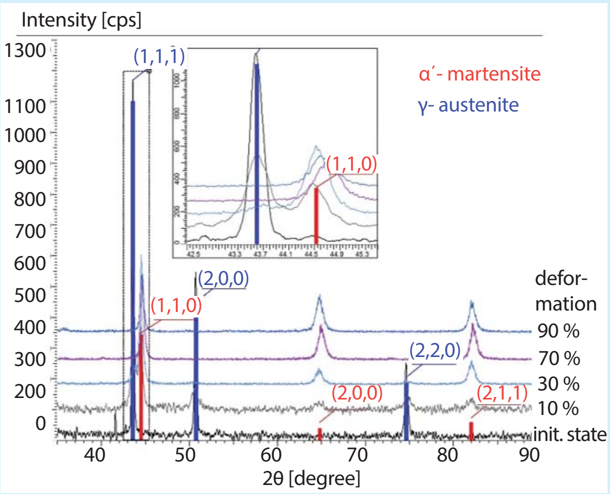

Fig. 1. Changes in the diffraction pattern of sample subjected to the longitudinal rolling up to different deformation degree

Results and discussion

Deformation

Diffraction patterns of samples rolled up to different deformation degrees are presented in **Fig. 1**. The patterns are shifted relative to each other along Y-axis for better visualization. We can see that phase composition of initial sample, consisting of only austenite, changes already at deformation of 10 % and α'-martensite arises. The shift of α'-martensite peak positions testifies about variation of lattice parameters. Approximately, at 50 % deformation the retained austenite completely disappears (**Fig. 2*a***).

We can see that in the deformation range 20–60 % the variation of FWHM of α'-phase reflections (Fig. 2*b*) has non-monotonic character which indicates the inhomogeneous formation of α'-martensite under cold deformation and the occurrence of two opposite processes in the martensite phase – hardening and softening under rolling within the double phase state.

The initial samples are characterized by very weak texture, what can be seen by texture index almost equal to unity (Fig. 2*c*). With an increase in the degree of deformation, the texture of the retained austenite becomes sharper. A formation of the martensite's typical rolling texture starts

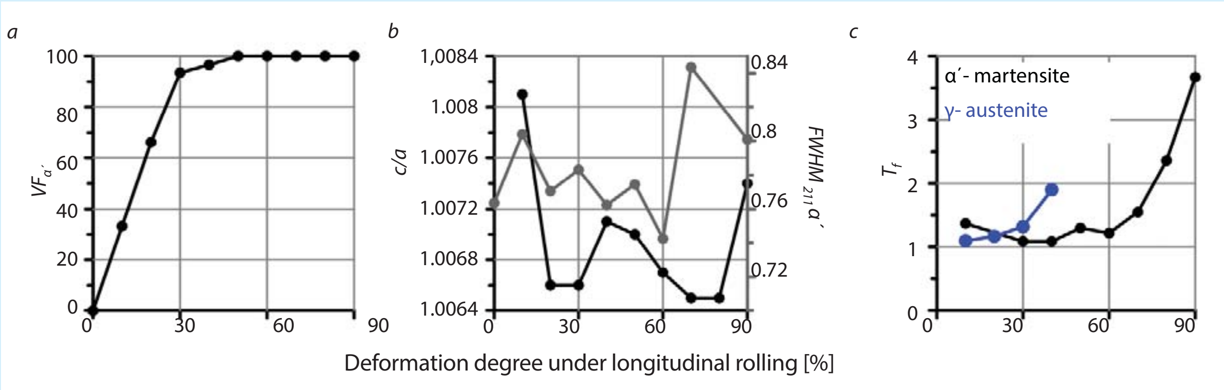

Fig. 2. Dependencies of $VF_{\alpha'}$ (*a*), the martensite's FWHM$_{\alpha'(211)}$ (*b*) and T_f (*c*) on the deformation degree for longitudinal rolling

only after disappearing of the austenite at the deformation of 70 %.

Thereby, in the presence of the γ-phase, a rather scatter texture of the α'-phase (T_f near 1) is observed up to 60 % deformation. The formation of the rolling texture begins only at the 70 % deformation and it seems to be insufficiently strong compared to the rolling of a single-phase BCC steel.

Heat treatment

Heat treatment results in the reverse α' → γ phase transformation that one can see in **Fig. 3**. The orientation relations of phase transformation depends on the deformation scheme – in the case of longitudinal rolling we see the abrupt intensity increasing of the (220) austenite reflection with the (200) decreasing of martensite already after 1 min holding time, while for cross-rolling more gradual intensity growth of austenite reflections is typical with the maintenance of (200)–martensite intensity. Thus, the character of orientation relations under α'→γ phase transformation is controlled by the deformation textures and deformation history and will be discussed further.

Fig. 4 shows the texture changes of samples deformed via longitudinal and cross-rolling during heat treatment. The martensite's texture after LR is typical for rolling texture of materials with BCC and BCT, characterized by the {001–112}<110> + {111}<112> + {554}<225> components. In the case of cross-rolling the final texture of α'-phase is rather different and its main components are {001}<110> and weaker {111}{110–112}. The CR reduces the fraction of the <110>‖RD component in the deformed state and strengthens its component {001}<110> with some scattering along φ_1, what similar to the forming of a fiber texture component {001}‖RP.

We can see that both phases, martensite and austenite, are subjected to texture changes after heat treatment. The main difference in the arising austenite texture is the presence of few components, which are {113}<332> and {110}<001–112>, in the case of longitudinal rolling and single component {110}<334> in the latter.

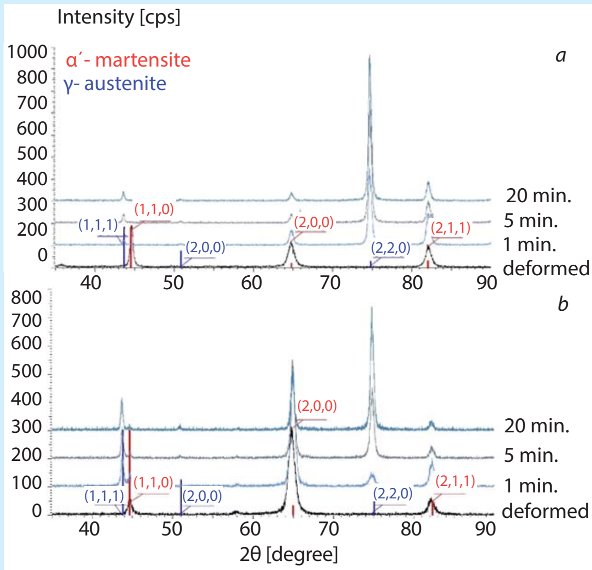

Fig. 3. Changes in the diffraction patterns of samples deformed up to 90 % via longitudinal (*a*) and cross-rolling (*b*) after different HT

At the same time the martensite texture under HT of CR samples changes while the ratios of different components fractions of LR samples is almost stable. In Fig. 4 one can also see the difference diagrams, constructed by the point-by-point subtraction of ODF for deformed sample from the annealed ($ODF_{HT} – ODF_{def}$). These diagrams show that single texture component of austenite in the CR samples arises mainly from the martensite component {001}<110> (blue regions of the diagram) while in the LR samples the main negative regions of the diagram are near texture components {111}<110-112> and {112}<110>.

Nowadays it is widely acknowledged [18, 19] that austenite → martensite orientation relationships (ORs) do not correspond exactly to either Kurdjumov-Sachs (K-S) or Nishiyama–Wassermann (N-W) but lay somewhere

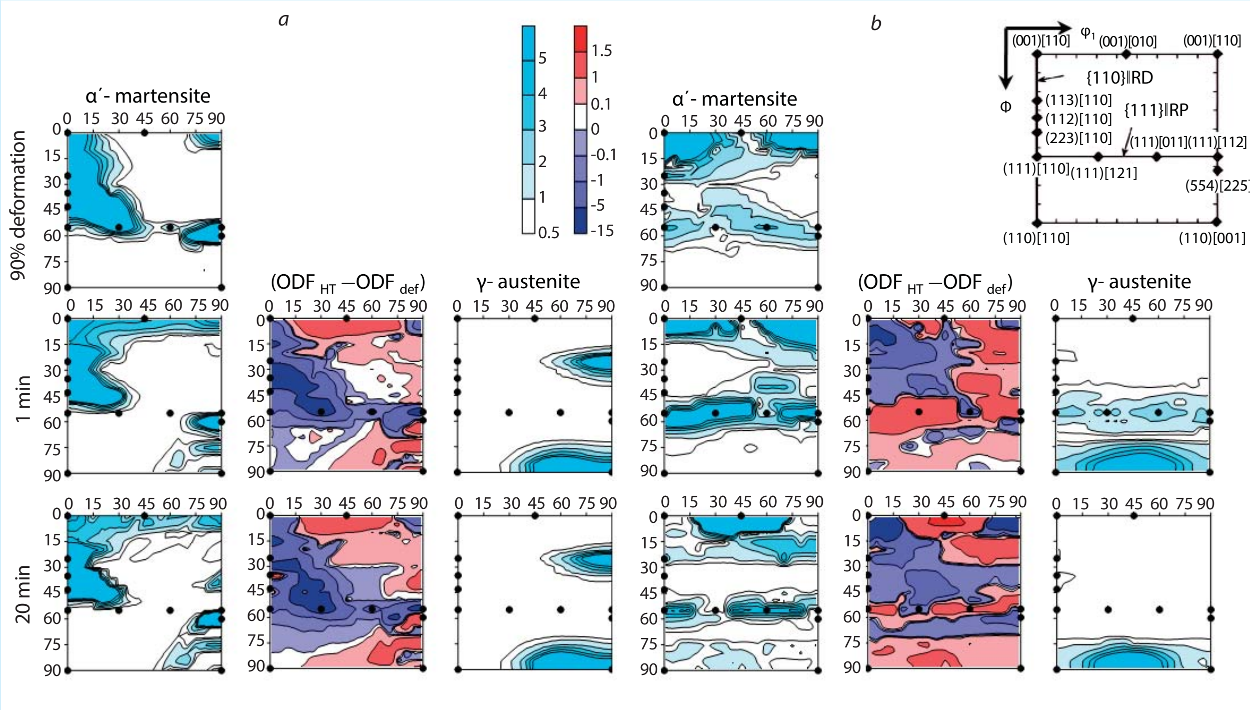

Fig. 4. Texture changes under heat treatment of samples deformed up to 90 % via longitudinal (*a*) and cross-rolling (*b*)

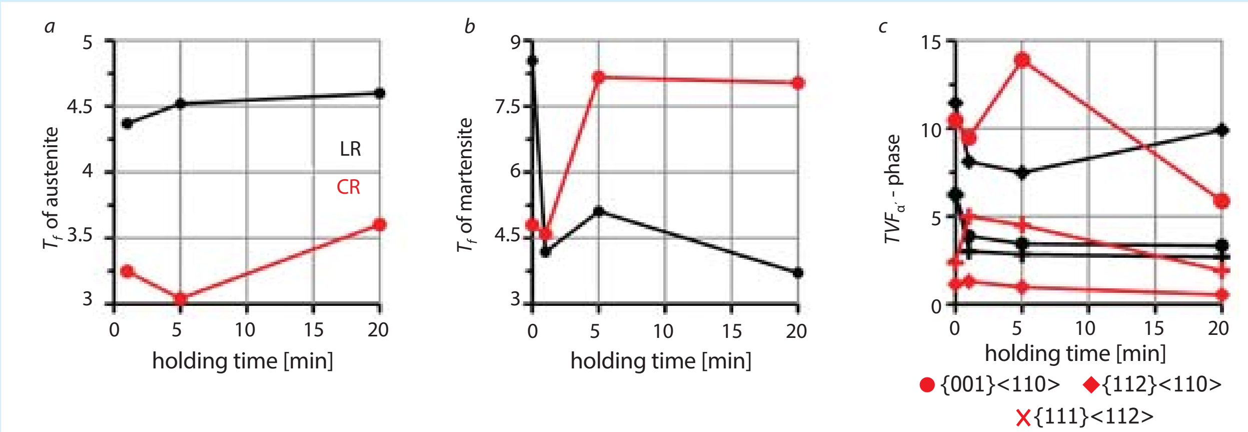

Fig. 5. The holding time dependencies of T_f for γ- (*a*) and α'-phases (*b*) and *TVF* of different components of α'-phase (*c*) constructed for LR (black lines) and CR (red lines) samples

between them. Thus, it seems that the orientation of reversed austenite for LR samples follows few among 24 variants of K-S ORs: $\{110\}_{\alpha'}\|\{111\}_{\gamma}$ and $<111>_{\alpha'}\|<110>_{\gamma}$. We also can reveal the following orientation relations for α' → γ phase transformation under heat treatment of CR samples: $\{100\}_{\alpha'}\|\{110\}_{\gamma}$ and $<110>_{\alpha'}\|<334>_{\gamma}$ with misorientation angle about 45 °. This distinction appears to be due to the different texture formation history and substructural state of grains attached to different texture components [20, 21].

Despite the multicomponent character, the texture of arising γ-phase in the case of LR samples is stronger, what T_f in **Fig. 5** indicates together with the texture scattering of retained α'-phase. From the same figure, it is seen that for LR samples TVFs of main texture components decrease simultaneously while in CR-samples only the {001}<110> volume fraction reduced.

From the **Fig. 6** (*a*) one can see that the holding time graph of $VF_{\alpha'}$ do not strongly depend on the deformation scheme and follow the conventional conception as well as the FWHM of α'-phase reflections (*b*). However the FWHM of γ-phase reflection (*c*) has higher values for CR samples, what results in the higher microhardness Fig. 6 (*d*) and lower plasticity (*e*). We can see that the plastic-

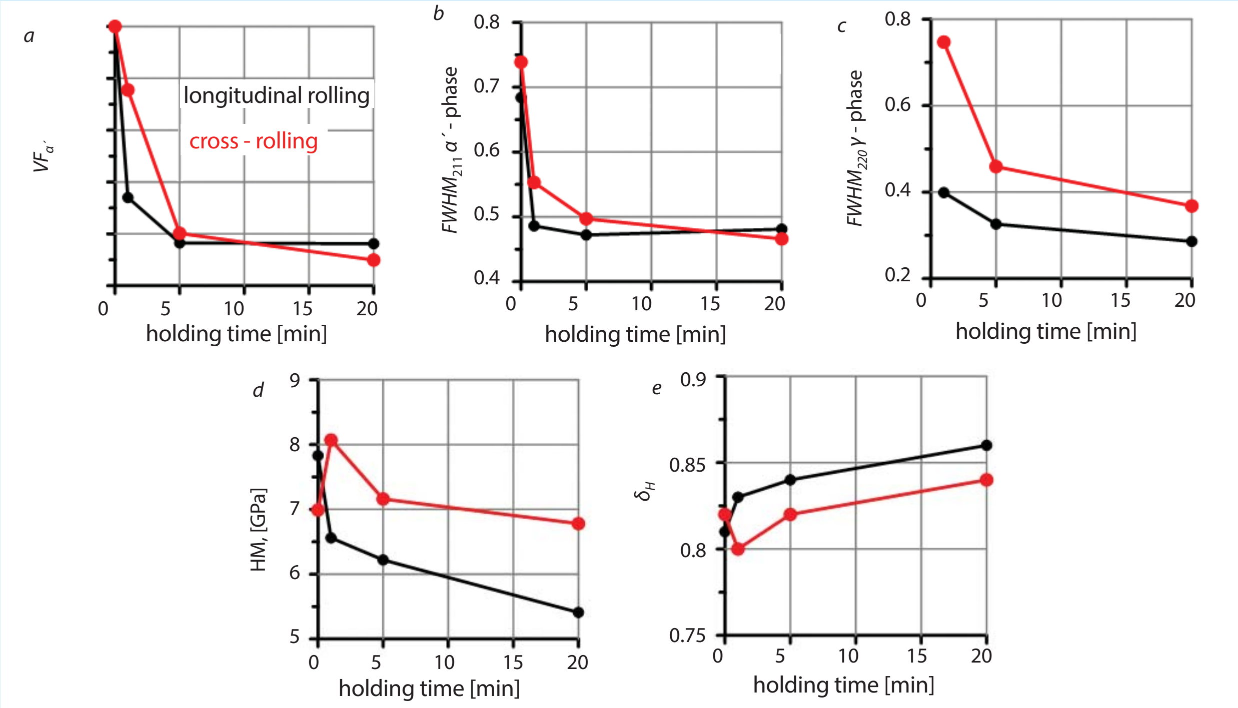

Fig. 6. The holding time dependencies of $VF_{\alpha'}$ (*a*), *FWHMs* of α'- (*b*) and γ-phases (*c*) and microhardness (*d*) and plasticity (*e*) of samples

ity for CR samples is lower approximately for 2.5 % than for LR while the microhardness increased for about 25 % after preheating of 20 min. Thus, the deformation scheme has a great influence on the texture development as well as on mechanical properties of the material. The abrupt rise in microhardness after 1-minute HT we can explain by the arising of fine-dispersed nuclei of austenite in the martensite grains with stronger texture, which strengthen the material. But the longer holding times results in the growth of austenites' grains and the material's softening. Therefore, the substructure and preferred orientation of reversed austenite, which initially depends on deformation process, define the mechanical properties of the material and should effect their anisotropy.

On the basis on the results totality we can conclude that the austenite formation in the longitudinally rolled samples occurs mainly at the expense of texture components {111}<112> of martensite and additionally {112}<110>, while in the case of the cross-rolling the mainly decreased martensite component is {001}<110>. At the same time, the more scattered martensite's deformation texture results in the fine-dispersed austenite formation after HT, which hardens the material with maintaining a high level of plasticity. This difference needs latter studies of substructural inhomogeneity [20, 21].

Conclusions

As a result of the research carried out, the following conclusions were made:

1) In the process of cold rolling, the γ → α'-martensite phase transformation is activated and at 50 % of cold deformation austenite completely disappears.

2) In the presence of an additional phase, the texture of both α'-martensite and austenite is rather scattered during rolling. Only after 50 % degree of deformation the {001–112}<110> martensite's texture component sharpens, which contributes to an increase in the properties anisotropy of the material. Under cross-rolling the main texture component of martensite is {001}<110>.

3) Heating before quenching of LR samples initiates the reverse α' → γ phase transformation with the formation of austenite texture {113}<332>+{110} <001–112>, which proceeds in accordance with the OR near K-S. CR samples is characterized only by single texture component {110}<334> after heat treatment. The texture sharpness of austenite is higher for the LR samples while for retained martensite the sharper texture is typical for CR samples.

4) The deformation scheme has a significant effect on texture texture development and mechanical properties. The formation of fine-dispersed austenite during heat treatment after cross-rolling, which hardens the material, is promoted by the scattering of the martensite's deformation texture.

Acknowledgments

The work was carried out with the financial support of the Ministry of Science and Higher Education of Russian Federation (Agreement No. 075-15-2021-1352).

REFERENCES

1. Guo X., La P., Li H., Wei Y., Lu X, Effect of the Deformation Amount on the Microstructure and Tensile Properties of 304 Stainless Steel with 2 wt% Al Content by Cold Rolling. *Steel Research International*. 2020. Vol. 91. pp. 2–10. DOI: 10.1002/srin.201900585.
2. Sun G., Du L., Hu J., Zhang B., Misra R. D. K. On the influence of deformation mechanism during cold and warm rolling on annealing behavior of a 304 stainless steel. *Materials Science and Engineering A*. 2019. Vol. 746. pp. 341–355. DOI: 10.1016/j.msea.2019.01.020.
3. Talonen J., Hänninen H. Formation of shear bands and strain-induced martensite during plastic deformation of metastable austenitic stainless steels. *Acta Materialia*. 2007. Vol. 55. pp. 6108–6118. DOI: 10.1016/j.actamat.2007.07.015.
4. Shen Y. F., Li X. X., Sun X., Wang Y. D., Zuo L. Twinning and martensite in a 304 austenitic stainless steel. *Materials Science and Engineering A*. 2012. Vol. 552. pp. 514–522. DOI: 10.1016/j.msea.2012.05.080.
5. Mumtaz K., Takahashi S., Echigoya J., Zhang L., Kamada Y., Sato M. Temperature dependence of martensitic transformation in austenitic stainless steel. *Journal of Materials Science Letters*. 2003. Vol. 22. pp. 423–427. DOI: 10.1023/A:1022999309138.
6. Naghizadeh M., Mirzadeh H. Microstructural Evolutions During Annealing of Plastically Deformed AISI 304 Austenitic Stainless Steel: Martensite Reversion, Grain Refinement, Recrystallization, and Grain Growth. *Metallurgical and Materials Transactions A: Physical Metallurgy and Materials Science*. 2016. Vol. 47. pp. 4210–4216. DOI: 10.1007/s11661-016-3589-1.
7. Isaenkova M., Perlovich Yu., Fesenko V., Dobrokhotov P., Tselishchev A., Changes of structure and crystallographic texture of cladding tubes from austenitic steel under thermal creep testing. *IOP Conference Series: Materials Science and Engineering*. 2016. Vol. 130. DOI: 10.1088/1757-899X/130/1/012007.
8. Amininejad A., Jamaati R., Hosseinipour S. J. Achieving superior strength and high ductility in AISI 304 austenitic stainless steel via asymmetric cold rolling. *Materials Science and Engineering A*. 2019. Vol. 767. pp. 138433. DOI: 10.1016/j.msea.2019.138433.
9. Zheng C., Liu C., Ren M., Jiang H., Li L. Microstructure and mechanical behavior of an AISI 304 austenitic stainless steel prepared by cold- or cryogenic-rolling and annealing. *Materials Science and Engineering A*. 2018. Vol. 724. pp. 260–268. DOI: h10.1016/j.msea.2018.03.105.
10. Ma B., Li C., Wang J., Cai B., Sui F. Influence of asymmetric hot rolling on through-thickness microstructure gradient of Fe–20Mn–4Al–0.3C non-magnetic steel. *Materials Science and Engineering A*, 2016. Vol. 671. pp. 190-197.
11. Yakovleva A., Isaenkova M., Minushkin R. The effect of combined processing on residual stresses in the surface layer of power plant parts. *Materials*. 2022. Vol. 15. p. 420. DOI: 10.3390/ma15020420.
12. Isaenkova M., Perlovich Y., Fesenko V. Modern methods of experimental construction of texture complete direct pole figures by using X-ray data. *IOP Conference Series: Materials Science and Engineering*. 2016. Vol. 130. p. 012055. DOI: 10.1088/1757-899X/130/1/012055.
13. Pawlik K. LaboTex: The Texture Analysis Software. http://www.labosoft.com.pl.
14. Bunge H. J. Texture Analysis in Materials Science. Butterworth, London, UK. 1982. 59 p.
15. EN ISO 14577-1:2015. Metallic materials – Instrumented indentation test for hardness and materials parameters. Part 1-3. 2015.
16. Sakai M. Simultaneous estimate of elastic/plastic parameters in depth-sensing indentation tests. *Scripta Materialia*. 2004. Vol. 51. pp. 391–395. DOI: 10.1016/j.scriptamat.2004.05.018.
17. Xu G. T., Sun B., Qiao Y. K., Wang G., Zhao M. H. Characterization of the plasticity parameters of the surface-modified layer of 18CrNiMo7-6 alloy steel after carburizing heat treatment through the indentation method. *Journal of Materials Research and Technology*. 2021. No. 12. pp. 2307-2316. DOI: 10.1016/j.jmrt.2021.04.028.
18. Yardley V. A., Payton E. J. Austenite–martensite/bainite orientation relationship: Characterisation parameters and their application. *Materials Science and Technology*. 2014. Vol. 30. pp. 1125–1130. DOI: 10.1179/1743284714Y.0000000572.
19. Haghdadi N., Cizek P., Hodgson P. D., He Y., Sun B., Jonas J. J., Rohrer G. S., Beladi H. New insights into the interface characteristics of a duplex stainless steel subjected to accelerated ferrite-to-austenite transformation. *Journal of Materials Science*. 2020. Vol. 55 (6). pp. 5322-5339. DOI: 10.1007/s10853-020-04358-3.
20. Perlovich Y., Isaenkova M., Fesenko V., Krymskaya O., Dobrokhotov P. Practical applications of the method of generalized pole figures. *IOP Conference Series: Materials Science and Engineering*. 2015. Vol. 82. p. 012075. DOI: 10.1088/1757-899X/82/1/012075.
21. Perlovich Y., Isaenkova M., Krymskaya O., Dobrokhotov P. Conditions for development of regular structure by deformation of metal materials. *AIP Conference Proceedings*. 2019. 2113. 040007 (5 p.). DOI: 10.1063/1.5112541.